Inelastic hard rods in a periodic potential

Fabio Cecconi
INFM Center for Statistical Mechanics and Complexity, Piazzale Aldo Moro 2, 00185 Rome, Italy and Dipartimento di Fisica, Università La Sapienza, Piazzale Aldo Moro 2, 00185 Rome, Italy

Umberto Marini Bettolo Marconi
Dipartimento di Fisica, Università di Camerino and INFM, Via Madonna delle Carceri, 62032 Camerino, Italy

Fabiana Diotallevi
Dipartimento di Fisica, Università La Sapienza, Piazzale Aldo Moro 2, 00185 Rome, Italy

Andrea Puglisi
INFM Center for Statistical Mechanics and Complexity, Piazzale Aldo Moro 2, 00185 Rome, Italy and Dipartimento di Fisica, Università La Sapienza, Piazzale Aldo Moro 2, 00185 Rome, Italy

(Received 18 March 2004; accepted 22 June 2004)

A simple model of inelastic hard rods subject to a one-dimensional array of identical wells is introduced. The energy loss due to inelastic collisions is balanced by the work supplied by an external stochastic heat bath. We explore the effect of the spatial nonuniformity on the steady states of the system. The spatial variations of the density, granular temperature, and pressure induced by the gradient of the external potential are investigated and compared with the analogous variations in an elastic system. Finally, we study the clustering process by considering the relaxation of the system starting from a uniform homogeneous state. © *2004 American Institute of Physics.*
[DOI: 10.1063/1.1782812]

I. INTRODUCTION

Recently granular gases, i.e., a large number of macroscopic particles colliding with one another and losing a little energy at each collision, have been studied employing methods of statistical physics.[1–5] The main practical motivation to improve the understanding of the dynamical and static properties of these materials stems from their relevance in a variety of technological and industrial processes.[6] Granular materials also represent a new paradigm in the context of nonequilibrium statistical mechanics. In fact, they are open systems which can reach a nonequilibrium stationary state when the energy loss, determined by the dissipative interactions, is balanced by the work supplied by an external driving force.

A current problem in this field, motivated by a series of recent experiments and theoretical work, concerns the behavior of driven granular gases subject to spatially nonuniform conditions.[7–16] These conditions can be realized experimentally by shaking the gas in a container divided in a series of identical compartments connected by holes. The following phenomenology is observed: for strong shaking intensity the grains jump from one compartment to the other, whereas for weak shaking intensity, they tend to break the discrete symmetry of the system and fill preferentially only some compartments. Such a clustering occurs because the grains, unlike an ideal gas of molecules, can dissipate heat when colliding. Therefore a spontaneous increase of the number of particles within a given compartment entails more collisions and a consequent higher energy loss. Thus the capability for the particles to leave the compartment is strongly inhibited leading eventually to clustering.

In the present paper we consider a simple modeling of the multicompartment experiment, namely, a one-dimensional system of inelastic hard rods[17–20] driven by a stochastic thermostat and subject to an external time-independent periodic potential. As shown in our recent paper,[21] the one-dimensional geometry of the model not only minimizes the amount of computational effort but also allows performing analytical guesses concerning the relevant observables.

As a premise, we recall that in the case of elastic hard rods coupled to a stochastic heat bath and in the presence of a periodic external potential most of the equilibrium properties can be computed by using an exact functional relation, proved by Percus,[22] between an arbitrary external potential and the equilibrium average density profile. It is natural to ask how the behavior of the elastic system will be affected upon switching on the inelasticity of the collisions. The equilibrium state of the elastic hard-rod system is replaced by a corresponding nonequilibrium steady state of the inelastic system. The comparison between the properties of the two systems offers a useful procedure to understand the interplay between the inelasticity, the excluded volume effect, and the external potential. As we shall see below the model shows a variety of nonequilibrium states according to the values of the control parameters, such as the external potential, the density, and the driving force. These states range from spatially periodic configurations to nonperiodic configurations in agreement with the experimental findings.

The paper is organized as follows. In Sec. II, we introduce the model we employed to study the effects of compartments in granular gases and we briefly discuss the main fea-

ture of the dynamics. In Sec. III, we compare the steady state properties of the model against the corresponding properties of the equilibrium elastic system. In Sec. IV, we consider the relaxation and clustering properties of the system. Finally, conclusions are presented in Sec. V.

II. A MODEL OF DRIVEN GRANULAR GAS IN COMPARTMENTS

The main issue of the present paper is to study how the properties of a granular fluidized system are affected by the presence of a static external nonuniform potential. We will show that such a confining potential can enhance the tendency toward cluster formation, generating inhomogeneities similar to those observed in some real granular systems placed in compartments. The model studied consists of a set of N impenetrable particles of equal masses m and lengths σ, moving on a ring under the influence of the periodic potential $V(x)$. Two mechanisms control the energy of the particles: the interaction with heat bath and the collisions among the particles. The collisions are instantaneous and binary, and dissipate a fraction $(1-r^2)/2$ of the total kinetic energy of the pair (r being the coefficient of restitution). The heat bath, instead, supplies an amount of energy which prevents the system to come at rest. In this paper we employ, a stochastic energy source, namely, the thermostat, previously employed in Refs. 14, 18, 21, and 23. The coupling of the particles to the heat bath consists of the combination of a velocity dependent frictional force and a random kick. We first write the evolution equation for the generic particle i in the system when the collisions are not taken into account:

$$m\frac{d^2x_i}{dt^2}=-m\gamma\frac{dx_i}{dt}-V'(x_i)+\xi_i(t), \tag{1}$$

where x_i $(i=1,\ldots,N)$, γ, and $V'(x)$ indicate the position of particle i, the friction coefficient and the spatial derivative of the external static potential, respectively. The kicks $\xi_i(t)$, are distributed according to a Gaussian law characterized by

$$\langle\xi_i(t)\rangle=0$$

and

$$\langle\xi_i(t)\xi_j(s)\rangle=2m\gamma T_b\delta_{ij}\delta(t-s).$$

The temperature T_b determines the intensity of the heat bath.

The external potential has a spatial period L/M, where L is the system size and M is the number of potential wells (i.e., number of local minima) in the interval $[-L/2,L/2]$. Each well mimics, in our simulation, a compartment in Lohse's experiments.[9] The boundary conditions are assumed to be periodic. We found that a rather convenient potential to use in numerical experiment is that of Refs. 24 and 25:

$$V(x)=\frac{\exp\{\alpha\cos(2\pi xM/L)\}}{I_0(\alpha)}, \tag{2}$$

where the zeroth-order modified Bessel function,[26] I_0, in the denominator enforces the normalization condition $1/L\int_0^L dxV(x)=1$. The shape of the potential $V(x)$ depends upon the parameter α (Fig. 1): as it increases, the shape of the barriers becomes more squarelike, approximating the condition of walls.

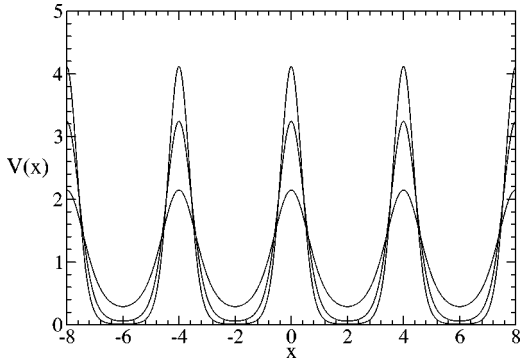

FIG. 1. Behavior of $V(x)$ for $\alpha=1,2,3$, as α increases, the barriers approximate the condition of walls and the wells become more squarelike.

Collisions redistribute the energy and the momenta among the particles. For a nearest neighbor pair a collision event takes place when the separation $x_{i+1}-x_i$ equals their length σ and determines a change of the velocities of the two particles according to the rule

$$v_i'=v_i-\frac{1+r}{2}(v_i-v_j), \tag{3}$$

where the prime indicates postcollisional variables. Notice that in the elastic case, $r=1$, the collisions do not change the total energy and that the average kinetic energy per particle attains asymptotically the value T_b. This state of affairs is altered for values of the coefficient of restitution less than 1 and the average kinetic energy per particle reaches [for $V(x)=0$] a value smaller than T_b.

In the following we will assume a unitary mass $m=1$.

The basic phenomenology of the inelastic model can be understood by considering the two competing effects controlling the dynamics: the hard-core interaction and the collisional dissipation. The former favors the equidistribution of the particles in the various wells, whereas the latter promotes the formation of clusters in some wells, thus breaking the periodic symmetry of the system. If the particles were independent, the passage from one well to the next would occur via an activated jump process, characterized by a typical exit time τ proportional to $\exp(\Delta V/T_b)$, where $\Delta V=2\sinh(\alpha)/I_0(\alpha)$ represents the energy barrier between adjacent wells. In other words, a local density excess of particles would be washed out by a diffusive process whose diffusion constant D has the Arrhenius dependence, $D=D_0\exp(-\Delta V/T_b)$ with $D_0=T_b/m\gamma$.

In a recent paper[14] we have shown that, in a granular toy model consisting of two wells and only two particles, two different jump processes can be clearly identified: the free jump, which occurs when the escape is from a singly occupied well, and the correlated jump, which occurs when the escape involves a doubly occupied well. The resulting scenario is that the jumping dynamics remains still Arrhenius-like but the jump rate strongly depends on the occupation of the well from which the jump occurs, i.e.,

$$\tau_k \propto \exp\left(\frac{\delta V_k}{T_k}\right), \tag{4}$$

where k indicates the occupation number ($k=1$ or 2). In the multiwell and many-particle systems, we shall discuss hereafter, the phenomenon is enhanced and the escape rate for a given well will depend on the number of particles inside that well.

The steady state properties of our model are investigated by means of molecular dynamics simulations of Eq. (1) for an ensemble of $N=1024$ hard particles of length $\sigma=0.2$ in a box of size $L=1024$. The heat-bath parameters are $\gamma=0.2$ and $T_b=1.0$. The potential constants $\alpha=1$ and $M=100$ imply 100 wells (compartments) of width $w=L/M=10.24$, separated by an energy barrier of height $\Delta V=1.856$. The computer implementation of the granular dynamics has been realized by a suitable modification of the event-driven algorithm to take into account the effects of the potential and of the heat bath. Particle positions and velocities within two consecutive collisions are updated according to a second-order discretization scheme for the dynamics, Eq. (1).

Simulations start from initial conditions corresponding to equally spaced nonoverlapping particles. After a transient time t_0, the system reaches a steady state characterized by robust statistical properties and one measures the generic observable $A(t)$ by performing the time average,

$$\langle A\rangle = \frac{1}{t-t_0}\int_{t_0}^{t} d\tau A(\tau), \tag{5}$$

over an appropriate interval $t-t_0$.

III. PROPERTIES OF THE STEADY STATE

We analyze first the reference elastic system ($r=1$) for which a true equilibrium state exists. Most of its properties are exactly known. For instance, the grand potential $\Omega[\rho(x)]$, from which all the equilibrium properties can be deduced, is a functional of the density $\rho(x)$ whose explicit form reads

$$\Omega[\rho] = T_b \int_{-L/2}^{L/2} dx \rho(x)\left[\ln\left\{\frac{\rho(x)}{1-\eta(x)}\right\} - 1 + \frac{V(x)-\mu}{T_b}\right]$$

with μ being the bulk chemical potential of the system and

$$\eta(x) = \int_{x-\sigma}^{x} ds \rho(s)$$

the local packing fraction. Extremizing $\Omega[\rho]$ with respect to $\rho(x)$ yields the following Euler-Lagrange equation:

$$\ln\frac{\rho(x)}{1-\eta(x)} = \beta[\mu - V(x)] - \int_{x}^{x+\sigma} dy \frac{\rho(y)}{1-\eta(y)}, \tag{6}$$

whose solution provides the equilibrium density profile. Notice that inserting this solution into Ω one obtains the value of the thermodynamic grand potential of the system,[27]

$$\tilde{\Omega} = -T_b \int_{-L/2}^{L/2} dx \frac{\rho(x-\sigma)}{1-\eta(x)}. \tag{7}$$

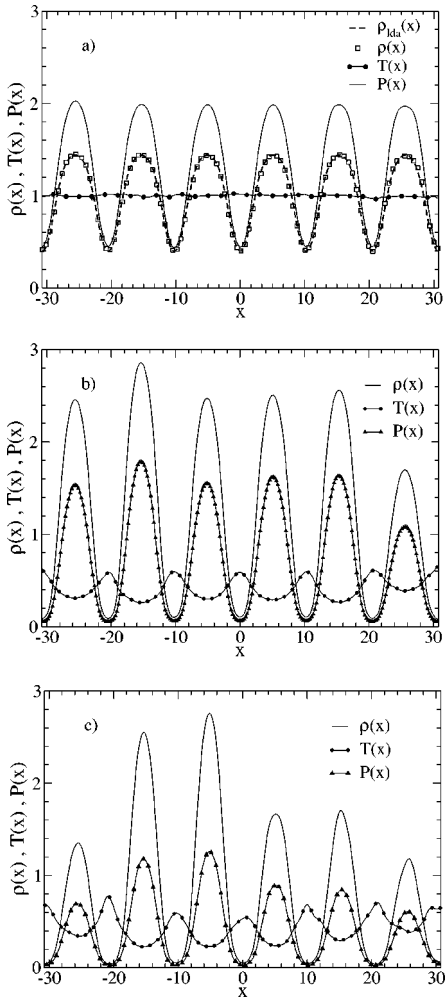

FIG. 2. Profiles of density, temperature, and pressure in a system of $N=1024$ rods, size $L=1024$, diameter $\sigma=0.2$, $M=100$ potential wells, and $r=1.0,0.8,0.6$ (a,b,c respectively). Notice that the granular temperature varies with the position and is anticorrelated with the density profile.

Using Eq. (7) in the uniform limit [$V(x)=0$], we obtain the bulk pressure $-\tilde{\Omega}/L = P = T_b\rho/(1-\rho)$.

Equation (6) can also be used to test the average profile obtained from the numerical solution of the dynamical equations. Since the potential $V(x)$ varies slowly over the hard-core diameter σ (i.e., $L/M \gg \sigma$), the Euler-Lagrange equation can be solved in the local density approximation (LDA),

$$V(x) + T_b\left\{\ln\left[\frac{\rho(x)}{1-\sigma\rho(x)}\right] + \frac{\sigma\rho(x)}{1-\sigma\rho(x)}\right\} = \mu. \tag{8}$$

The density profile $\rho_{LDA}(x)$ solving Eq. (8) is shown along with the corresponding quantity obtained from the numerical simulation in Fig. 2(a), and an excellent agreement is found. In the nonuniform case, the pressure is obtained from the hydrostatic equilibrium equation:

$$\frac{dP(x)}{dx} + \rho(x)V'(x) = 0. \tag{9}$$

As we shall see later the grand potential functional is related to the probability distribution of numbers of particles occupying each cell.

In the elastic system the temperature and the pressure can be obtained in two equivalent ways: the first is through their kinetic definition and the second via their thermodynamic definition. On the contrary in the inelastic system both quantities can be obtained only via their mechanical definitions. Then temperature is computed through the kinetic energy

$$T_g = m \sum_{i=1}^{N} \langle v_i^2 \rangle / N.$$

The pressure is evaluated by considering the impulse transferred across a surface in the unit of time[13,28] and is given by the sum of the ideal gas term $P_{id} = T_g \rho$ and the collisional P_{exc}:

$$P = \rho T_g(\rho) + \frac{\sigma}{L t_{ob}} \sum_{k=1}^{M_c} \delta p_k . \tag{10}$$

Here t_{ob} is the observation time, the sum runs over the M_c collisions occurring during T_{ob}, and $\delta p_k = m \delta v_k$ represents the impulse variation in the kth collision. As shown in Fig. 2(a), the pressure profile follows the same pattern as the density. Let us remark that with the parameters employed here the results of LDA are in fair agreement with the corresponding results of the simulations, thus suggesting that even in the inelastic case a treatment of the excluded volume effect as a local density effect might be appropriate.

Let us consider the effect of the inelasticity. In Figs. 2(b) and 2(c), obtained with $r = 0.8$ and $r = 0.6$, one observes two important features: the temperature profiles become nonuniform and the density ceases to be periodic. In fact, the kinetic temperature decreases in the more populated regions due to the higher collision rate. The particles being less energetic, when they belong to a cluster, tend to remain trapped even more in the wells.

Notice that the average pressure is lower than the corresponding pressure in the elastic system at the same average density due to the lower value of T_g with respect to T_b. It also varies from well to well, in apparent contradiction with the law of hydrostatic equilibrium. In fact, the state described by Figs. 2(b) and 2(c) is not stationary, but is associated with a very slow relaxation mode, i.e., with the large exit time τ from the wells.

At this point, it is interesting to discuss the existence of a relationship between the quantities ρ, P, and T in a granular gas, i.e., of an ''equation of state.'' In Fig. 3 we plot parametrically the numerical values of the pressure versus the density obtained by profiles in Fig. 2(a) for the elastic system. We notice the data are in good agreement with the exact Tonks formula,[29]

$$P(\rho) = T_b \frac{\rho}{1 - \sigma\rho}. \tag{11}$$

In a recent paper[21] we generalized expression (11) to the case of a granular system with no external potential and found

$$P(\rho) = T_g(\rho) \left[\rho + \frac{\sigma \rho^2}{1 - \sigma\rho} \right] = T_g(\rho) \frac{\rho}{1 - \sigma\rho}. \tag{12}$$

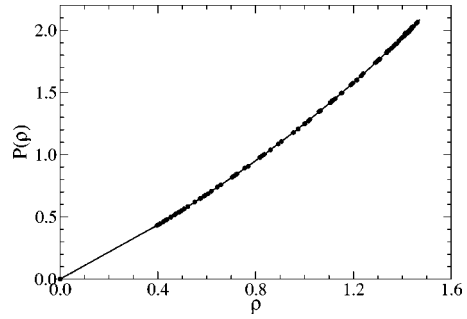

FIG. 3. Scatter plot of temperature and pressure vs density for the elastic system. Points are obtained by plotting data of Fig. 2(a) in a parametric plot $\{\rho(x), P(x)\}$ which eliminates the x dependence. Solid line indicates the exact result (11).

Equation (12) is equivalent to Eq. (11), upon replacing T_b with $T_g(\rho)$. The granular temperature is a function of the density since its value is determined by the balance between the average power dissipated in the collisions and the power supplied by the thermal bath. Therefore the larger the number of collisions (i.e., the larger the density) the lower is the granular temperature, which reads

$$T_g(\rho) = \frac{T_b}{1 + \dfrac{1 - r^2}{2\gamma} \dfrac{\rho}{1 - \sigma\rho} \sqrt{\dfrac{T_g}{m}}}. \tag{13}$$

Formulas (13) and (12) have been tested in the homogeneous case and shown to provide reasonable fits to the numerical data.[21]

In the inhomogeneous case $[V(x) \neq 0]$ with inelasticity $(r < 1)$, we extracted from the numerical simulations the density, temperature, and pressure profiles and drew the parametric plots shown in Figs. 4(a) and 4(b).

One observes that the plots deviate from the theoretical predictions and are more scattered. The reason for the breakdown of formulas (12) and (13) can be traced back to the inaccurate evaluation of the collision rate in the presence of the confining potential. The presence of the wells, indeed, strongly increases the collision rate at the bottom of each well, thus enhancing the effects of inelasticity.

IV. DYNAMICAL PROPERTIES

In this section we focus our attention on the clustering process which occurs spontaneously, starting from a uniform configuration, when the temperature of the heat bath is comparable with the energy of the potential barriers. Since the collisional cooling determines a decrease of the local temperature in the regions of high density, some compartments, randomly selected by the dynamics, may act as germs for the nucleation of a clustering process. Thus after a long transient, the occupation of few compartments may grow at the expense of the others which remain less densely populated.

An immediate and effective description of the clustering phenomenon can be achieved by analyzing the statistics of the occupation of the wells. We study the probability that the ith well is occupied by n_i particles. In the ideal gas (i.e.,

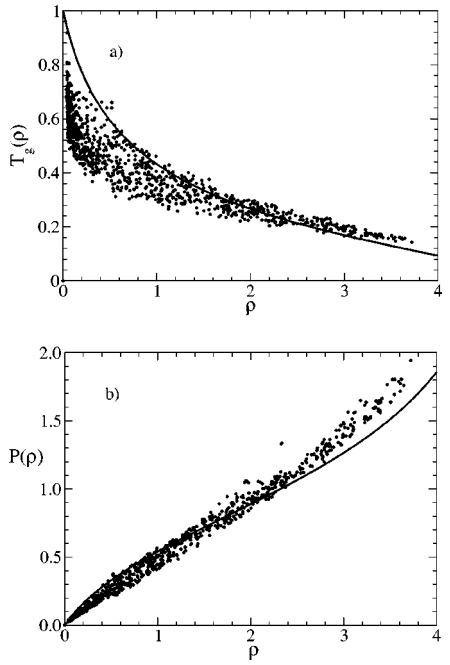

FIG. 4. Scatter plot of temperature (a) and pressure (b) vs density for a system with an inelasticity coefficient $r=0.6$. Points are obtained from the profile data of Fig. 2(c). Solid lines indicate the theoretical estimate for temperature (13) and pressure (12) derived in Ref. 21 for the system without potential. We notice the systematic deviation of the measured temperature from the theoretical estimate. Its origin is probably due to the large density fluctuations in the boundary regions separating the wells.

independent and identically distributed particles) the distribution function of N particles into M identical cells follows a Poisson law:

$$P(n_i)=\frac{\lambda^{n_i}\exp(-\lambda)}{n_i!}, \tag{14}$$

where $\lambda=N/M$ is the mean (also most probable) occupation value and the variance is $\sigma^2=pN=N/M=\lambda$. It is instructive, also in the light of the discussion below, to link the distribution (14) to the grand potential functional. Let us consider the probability of having a configuration with $n_1,n_2,\ldots,n_M$ particles in the M compartments:

$$\Pi[\{n_s\}]=\prod_{s=1}^{M} P(n_s). \tag{15}$$

For the equilibrium system we write

$$\Pi[\{n_s\}]=\mathcal{N}\exp(-\Omega[\{n_s\}]/T_b), \tag{16}$$

where $\mathcal{N}$ is a normalization factor and Ω indicates the ideal-gas coarse grained grand potential,

$$\Omega[\{n_s\}]=T_b\sum_{s=1}^{M}[n_s(\ln n_s-1)-\mu n_s] \tag{17}$$

The external potential, whose role is merely to confine the particles into the wells, has been eliminated replacing the original microscopic density field $\rho(x)$ with the coarse grained variables n_i. Finally, substituting Eq. (17) into Eq. (16) we find

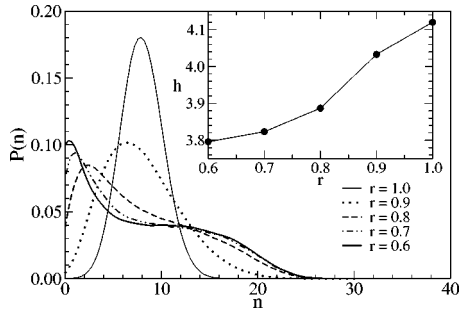

FIG. 5. Occupation probability of the wells for the elastic and inelastic system at different values of $r=1,0.9,0.8,0.7,0.6$, $M=64$ wells, and $N=512$ particles. Elastic curve has a Poisson-like shape, given by Eq. (21), peaked around the average occupation $\lambda=N/M=8$. Curves referring to inelastic system deviate from the elastic one. Inset: Entropic indicator h as a function of the inelasticity r.

$$\Pi[\{n_1\}]=\mathcal{N}\prod_{s=1}^{M}\frac{(e^{\mu/T_b})^{n_s}}{n_s!}, \tag{18}$$

which is identical to expression (15), provided λ is replaced by $e^{\beta\mu}$ and a suitable normalization factor $\mathcal{N}$ is chosen.

Such an ideal-gas formula has to be modified in the case of the elastic hard-rod system, because the hard-core repulsion induces correlations among the positions of the particles. The excluded volume constraint can be accounted for in a simple fashion by replacing the ideal-gas functional Ω by the corresponding hard-rod coarse grained functional:

$$\Omega_{hr}[\{n_s\}]=T_b\sum_{s=1}^{M}\left\{n_s[\ln n_s-1-\ln(N_m-n_s)]-\frac{\mu n_s}{T_b}\right\}, \tag{19}$$

where N_m is the maximum number of nonoverlapping rods which can occupy a single well. The extremization of Ω_{hr} with respect to n_s yields the link between the chemical potential μ, N_m, and the mean occupation λ:

$$\mu=T_b\left[\ln\lambda-\ln(N_m-\lambda)+\frac{\lambda}{N_m-\lambda}\right]. \tag{20}$$

In this case the distribution reads

$$\Pi_{hr}[\{n_s\}]=\mathcal{N}\exp(-\Omega_{hr}[\{n_s\}]). \tag{21}$$

It displays an enhancement and a narrowing of the peak centered at $\lambda=N/M$, because configurations characterized by highly populated compartments are unfavored (see Fig. 5). The narrowing of the peak can also be understood as a consequence of the lower compressibility of the hard-rod system with respect to the ideal one.

The presence of inelasticity introduces a different scenario with respect to the elastic case. Indeed, the energy dissipation strengthens the correlations and contrasts the hard-core repulsion. Then, as the inelasticity parameter r decreases, $P(n_i)$ deviates more and more from the elastic hard-rod distribution displaying a much larger variance, as shown in Fig. 5. The shape of $P(n_i)$ reflects the clustering tendency of the inelastic system, because a slower decay of P in the region $n_i>\lambda$ indicates the formation of clusters in few boxes. At the same time the peak of the distribution shifts to lower values of n_i, showing that the majority of the

compartments are nearly empty: we observe many wells containing just a small number of particles ($n_i \ll \lambda$) and few highly populated wells, in contrast with the elastic case.

The clustering phenomenon is well represented by the following statistical indicator:

$$h = -\sum_{i=1}^{M} \frac{n_i}{N} \ln \frac{n_i}{N}. \tag{22}$$

The usefulness of h in characterizing inhomogeneous particle distribution in compartments is illustrated by considering the two limiting cases. When all particles pile up into a single well, $h \to 0$ (minimum value), whereas h takes on its maximum value, $\ln(M)$, when all the M wells have identical populations. In intermediate cases, the quantity $F = \exp(h)$ represents a measure of the average number of occupied compartments. In the inset of Fig. 5 we report the asymptotic value of h as a function of r referring to a system of $N = 512$ particles and $M = 64$ compartments. The value of h decreases monotonically as the system becomes less elastic, indicating that the grains tend to group together, reducing in this way the fraction of occupied wells. Notice that as $r \to 1$ the entropic indicator is slightly larger than the value $h_R = 4.0957$ concerning a Poisson distribution with the parameter tuned to the simulation setup ($\lambda = N/M = 8$). This discrepancy is a consequence of excluded volume effects that result in the narrowing of the distribution $P(n_i)$ discussed above [Eq. (21)]. The onset of clustering regimes can be emphasized by the time evolution of h and by making the direct comparison between the elastic and inelastic cases (see Fig. 6). The system is initially prepared in a state where the grains are nonoverlapping and uniformly distributed among the $M = 10$ compartments. Their velocities are drawn according to a Maxwell distribution at the temperature T_b of the heat bath. The dynamics drives the system toward a new set of configurations.

Figure 6 shows that h (dots) for elastic particles fluctuates around a constant value which is very close to the equipopulated limit $\ln(M)$ indicated by the dashed line: as expected, there is no evidence of clustering in the elastic system. On the other hand, the clustering clearly appears from the curves of $h(t)$ referring to the inelastic system with $r = 0.8$. After a transient regime, the indicator $h(t)$ becomes stationary, fluctuating around a value which is considerably lower than the one corresponding to $r = 1$. This means that, due to clustering, only few wells result to be effectively populated. The time at which the inelastic system departs from homogeneity depends crucially on the number of particles, as illustrated in Fig. 6 at $N = 64$ and $N = 128$. We notice that the clustering cannot be considered complete because h does not vanish but displays small fluctuations around a small constant value. This implies that clusters exist as dynamical structures, where particles can enter and exit. Otherwise, it may even happen that a cluster already formed in a well breaks and reforms into another well after a long time. However, Fig. 6 shows that the observable $h(t)$ is a meaningful indicator, because it reaches a statistically steady value even when $\rho(x,t)$ is not fully stationary (as discussed in the preceding section). We stress that if one performs an average of $\rho(x,t)$ in a time larger than the maximum escape

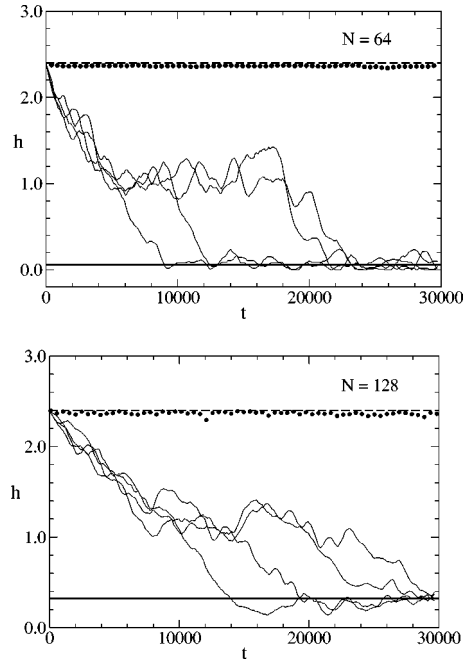

FIG. 6. Evolution of the entropic parameter h for a system starting from a uniform configuration (equipopulated wells) with $N = 64$, $N = 128$ particles of size $\sigma = 0.1$, $M = 11$ wells of width 15.0 (density $= 0.775$), parameter $\alpha = 8.0$, and energy barriers 3.486. The dashed reference line represents the uniform occupation $\ln(M)$, the points correspond to the elastic system ($r = 1$), while the lower four curves refer to different initializations of velocities from a Maxwell distribution at temperature $T_b = 2$ and inelasticity $r = 0.8$. Thick horizontal line indicates the average of the asymptotic h values over 40 runs.

time, the profile $\overline{\rho(x,t)}$ would appear spatially uniform, while $h(t)$ for any time t (after the initial transient) indicates that the density is *nonuniform*. Therefore h has to be considered the correct order parameter to characterize density inhomogeneities in the system.

Now, we turn our attention to a different process: we consider the evolution of an initial clustered configuration, where all the N particles at $t = 0$ are located inside a central compartment in a system made of $M = 3,5,7,9,15$ wells.[30] We expect, according to the level of the heat-bath temperature T_b, two different regimes: (i) for large T_b the cluster decays toward the fully equidistributed state $n_i = N/M$ and $\lim_{t \to \infty} F(t) = M$, since particles tend to fill neighboring cells and distribute all over the system; (ii) for low T_b the occupation of the compartment remains almost constant. It is useful to define a characteristic time t_s, as the shortest time required by the population of the central well, $n_0(t_s)$, to reach the fully equidistributed value $\lambda = N/M$. Unlike the mean-field predictions,[9,16] such a lifetime is a strongly fluctuating variable, depending on the initial configurations and on the "noise" history. Therefore we computed its average $\tau = \langle t_s \rangle$ over 100 different runs and different number of wells. The results are reported in Fig. 7 where the average lifetime τ is plotted against the inverse of the heat-bath temperature. We observe the Arrhenius-like behavior[14] with slopes changing with the total number of boxes M, in qualitative agreement with the analytical predictions.[9,16] The larger the number of wells, the smaller is the slope, indicat-

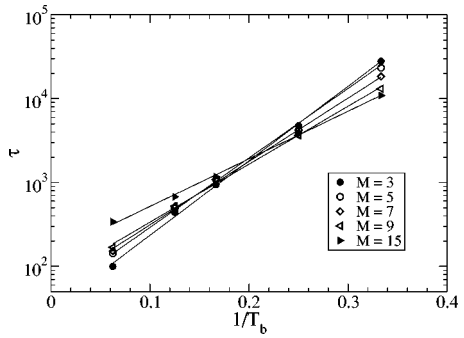

FIG. 7. Average lifetime τ of a cluster initially placed in the central well as a function of the heat-bath temperature T_b ($\gamma=0.2$) at different numbers $M=3,5,7,9,15$ of wells, each of size 20.0. The average has been performed over a set of 100 randomly selected initial configurations in a granular system with $N=128$ particles of $\sigma=0.1$ and $r=0.7$, with $\alpha=8$ and potential barrier $\Delta V=3.486$.

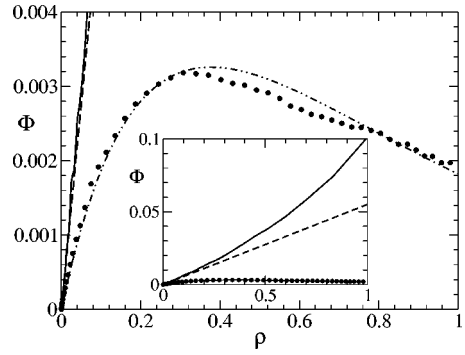

FIG. 8. Flux vs density for a single potential well ($M=1$) with absorbing boundaries. The curves refer to independent (dashed), elastic (full), and inelastic (circles) particles. Simulations parameters are initial occupation number $N=50$, $\sigma=0.1$, $\alpha=8$, well size $w=50$ (barrier $\Delta V=3.486$), bath temperature $T_b=1.0$, and coefficient of restitution $r=0.8$. The theoretical prediction of the flux described in the Appendix is the dot-dashed plot. The inset reports the same curves on a larger scale.

ing that the most stable cluster is the one with only three wells. We also remark that we were not able to observe a sudden death of the cluster as predicted by theoretical approaches.

Among the theoretical treatments of compartmentalized granular gases, the flux model[8–11,31] enjoys a great popularity in view of its simplicity. At the heart of this approach is the so-called flux-function $\Phi(n)$, which represents a measure of the number of particles crossing a section of the system per unit time. The form of the flux function is admittedly phenomenological and follows from the experimental observations. The latter requires $\Phi(n)$ to be, at fixed driving intensity, an increasing function for moderate values of the occupation number, n, and a decreasing function for larger values of n, to account for the stronger dissipation at high densities. Such a nonmonotonicity entails the possibility of spatially nonuniform steady solutions.[9]

For the sake of comparison, we extract from simulations the flux function for our model, by measuring the number density of particles, ρ, flowing outside a given well per unit time as a function of the density of particles within that well. The simulations start from an initial configuration where all the $N_0=50$ particles are located in the same well of width $w=25$ ($\rho_0=N_0/w$) and height $\Delta V=3.486$. Once the particles reach the top of the barrier, they are not allowed to reenter (absorbing boundary conditions). As time goes on, we record the density $\rho_{out}(t)$ of particles escaping from the well and average it over an ensemble of 1000 randomly selected initial configurations. The averaging procedure yields a curve $\langle\rho_{out}(t)\rangle$ from which we estimate its time derivative numerically. Finally, a parametric plot of $d\langle\rho_{out}(t)\rangle/dt$ versus the density of the remaining particles in the well, $\rho_0-\langle\rho_{out}(t)\rangle$, gives the flux function $\Phi(\rho)$ of the model. It is instructive to compare the properties of the flux relative to three different systems: noninteracting, elastically colliding, and inelastically colliding particles, as shown in Fig. 8. In the low density limit the interactions are almost negligible and the flux functions display a linear behavior characterized by a common slope. The situation becomes more interesting when the well contains more particles. The flux for noninteracting particles grows linearly with ρ (dashed curve): the larger the ρ, the larger is the probability to observe an escape event. While, in the system of elastic hard particles, the hard-core potential produces two competing effects: on one hand the repulsion makes the escape rate for particles near the border of the well larger than the corresponding rate for noninteracting particles. On the other hand, the same repulsion induces a cage effect entrapping the inner particles and tends to reduce the escape rate. However, from the dot-dashed curve in the inset of Fig. 8, we see that the first effect overcomes the second enhancing the flux with respect to independent particles. Finally, in the inelastic case, the tendency of the particles to form clusters and to dissipate kinetic energy greatly decreases the exit probability from the well, so that the flux is much smaller (almost two orders of magnitude) than the flux for the independent and elastic systems. We observe a slow increase with ρ and a local maximum clearly visible in dot curve of Fig. 8. The dot-dashed line, in the same figure, represents instead the theoretical attempt to explain the behavior of $\Phi(\rho)$ through a Kramers' theory which combines the excluded volume effect and the inelasticity into the escape-time formula (4) (see Appendix). The theoretical curve is plotted for all the same parameters of the simulations except for a unknown prefactor which is used as a fitting coefficient.

V. CONCLUSIONS

In this paper, inspired by a series of recent experiments, we have introduced and studied a model of randomly driven inelastic hard rods in the presence of an external spatially periodic potential. The one-dimensional model presents some of the salient features of higher dimensional models, such as packing, clustering and velocity correlations.[21] By comparison with the elastic hard-rod model, used here as reference system, we found that the inelasticity has deep repercussions on the configurational properties. The fluctuations in the density result to be increased and show the tendency of the system to cluster. Moreover, the (granular) temperature profile ceases to be spatially uniform showing minima in correspondence of the density maxima. As a mea-

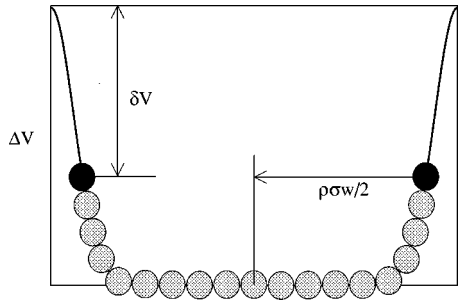

FIG. 9. Sketch of the reduction in the barrier height due to the excluded volume effect and leading to the renormalized flux function (A2).

sure of the density fluctuations we have introduced an ''entropic'' indicator h which provides information about the statistics of the partition of the grains in the various wells. We also performed numerical experiments concerning the stability of a cluster obtained by initially concentrating all the particles in a single well. Finally, we considered within the model the shape of the flux function which plays a major role in the macroscopic description of compartmentalized systems.

ACKNOWLEDGMENTS

We thank Massimo Cencini for very useful discussions and suggestions. U.M.B.M. acknowledges the financial support by COFIN-MIUR, Grant No. 2003020230, and F.C. acknowledges the financial support by FIRB-MIUR, Grant No. RBAU013LSE-001.

APPENDIX: FLUX FUNCTION

In this appendix we present a theoretical argument to explain the behavior of flux function Φ measured in simulations. The flux of particles outside of a potential well, with size w, height ΔV, and populated with a density ρ, can be computed via the formula

$$\frac{d\rho}{dt} = \Phi(\rho) = \frac{\rho}{\tau(\rho)}, \tag{A1}$$

where $\tau(\rho)$ is the particle escape time across the barrier. For the present granular system, this time follows the Kramers-Arrhenius law for independent particles, but with parameters renormalized by interactions. As already mentioned, $\tau(\rho)$ is the outcome of two competing effects, the excluded volume and the granular dissipation. The dissipation determines the granular temperature that can be approximated by the solution of Eq. (13), which holds only for an inelastic system without external potential. However for the potential parameters chosen in our simulations, formula (13) can be considered a fair approximation of the temperature in a well, because wells are rather flat and barriers so steep that particles feel the confining effect of the potential only in the neighborhood of well boundaries (Fig. 9). The excluded volume interaction, instead, is responsible for a mean reduction of the potential barrier ΔV. This effect is pictorially illustrated in Fig. 9, where the left-most/right-most particles (darker), the only ones allowed to jump, are displaced from the well center x_c of an amount $\rho\sigma w/2$. They experience an effective energy barrier roughly estimated as

$$\delta V(\rho) = V(x_c + w/2) - V(x_c + \rho\sigma w/2) \tag{A2}$$

and the renormalized Arrhenius law becomes

$$\tau(\rho) = \frac{1}{\nu}\exp\{\delta V(\rho)/T_g(\rho)\}. \tag{A3}$$

Simulations indicate a very weak dependence of ν on ρ for the parameters we employed. Therefore, the prefactor ν^{-1} has been considered as an adjustable time scale. Numerical solutions of Eq. (13) computed at different densities allow to construct the curve of the flux Φ as a function of ρ, reported in Fig. 8 in dot-dashed style.

[1] *Granular Gas Dynamics*, Lectures Notes in Physics Vol. 624, edited by T. Pöschel and N. Brilliantov Springer, (Berlin, 2003), and references therein.
[2] L. P. Kadanoff, Rev. Mod. Phys. **71**, 435 (1999).
[3] H. M. Jaeger and S. R. Nagel, Science **255**, 1523 (1992); H. M. Jaeger, S. R. Nagel, and R. P. Behringer, *ibid.* **68**, 1259 (1996).
[4] I. Goldhirsch, Annu. Rev. Fluid Mech. **35**, 267 (2003).
[5] I. Goldhirsch and G. Zanetti, Phys. Rev. Lett. **70**, 1619 (1993).
[6] *Powders and Grains 97*, edited by R. P. Behringer and J. T. Jenkins (Balkema, Rotterdam, 1997).
[7] H. J. Schlichting and V. Nordmeier, Math. Naturwiss. Unterr. **49**, 323 (1996).
[8] J. Eggers, Phys. Rev. Lett. **83**, 5322 (1999).
[9] D. van der Meer, K. van der Weele, and D. Lohse, Phys. Rev. E **63**, 061304 (2001).
[10] K. van der Weele, D. van der Meer, and D. Lohse, Europhys. Lett. **53**, 328 (2001).
[11] D. van der Meer, K. van der Weele, and D. Lohse, Phys. Rev. Lett. **88**, 174302 (2002).
[12] J. Javier Brey, F. Moreno, R. García-Rojo, and M. J. Ruiz-Montero, Phys. Rev. E **65**, 011305 (2002).
[13] A. Barrat and E. Trizac, Mol. Phys. **101**, 1713 (2003).
[14] F. Cecconi, A. Puglisi, U. Marini-Bettolo-Marconi, and A. Vulpiani, Phys. Rev. Lett. **90**, 064301 (2003); U. Marini-Bettolo-Marconi, F. Cecconi, and A. Puglisi, Proceedings of ''Traffic and Granular Flows 2003,'' Delft.
[15] U. Marini-Bettolo-Marconi and A. Puglisi, Phys. Rev. E **68**, 031306 (2003).
[16] U. Marini-Bettolo-Marconi and M. Conti, Phys. Rev. E **69**, 011302 (2004).
[17] N. Sela and I. Goldhirsch, Phys. Fluids **7**, 507 (1995).
[18] D. R. M. Williams and F. C. MacKintosh, Phys. Rev. E **54**, R9 (1996).
[19] S. McNamara and W. R. Young, Phys. Fluids A **4**, 496 (1992); *ibid.* **5**, 34 (1993).
[20] Y. Du, H. Li, and L. P. Kadanoff, Phys. Rev. Lett. **74**, 1268 (1995).
[21] F. Cecconi, F. Diotallevi, U. Marini-Bettolo-Marconi, and A. Puglisi, J. Chem. Phys. **120**, 35 (2004).
[22] J. K. Percus, J. Stat. Phys. **15**, 505 (1976).
[23] S. J. Moon, M. D. Shattuck, and J. B. Swift, Phys. Rev. E **64**, 031303 (2001).
[24] M. O. Magnasco, Phys. Rev. Lett. **71**, 1477 (1993).
[25] A. C. Branka, A. K. Das, and D. M. Heyes, J. Chem. Phys. **113**, 9911 (2000).
[26] M. Abramowitz and I. Stegun, *Handbook of Mathematical Tables* (Dover, New York, 1964).
[27] E. Roman and W. Dieterich, Phys. Rev. A **32**, 3726 (1985).
[28] M. P. Allen and D. J. Tildesley, *Computer Simulation of Liquids* (Clarendon, Oxford, 1987).
[29] L. Tonks, Phys. Rev. **50**, 955 (1936).
[30] We properly shift the potential to bring the minimum of the central well to coincide with the origin of x axis: $V(x) \to V(x - w/2)$.
[31] F. Coppex, M. Droz, and A. Lipowski, Phys. Rev. E **66**, 011305 (2002).